Available online at www.sciencedirect.com
SCIENCE DIRECT®
International Journal of Heat and Mass Transfer 47 (2004) 827–841
International Journal of HEAT and MASS TRANSFER
www.elsevier.com/locate/ijhmt

A parameter estimation approach to solve the inverse problem of point heat sources identification

Christophe Le Niliot [a,*], Frédéric Lefèvre [b]

[a] Laboratoire IUSTI, UMR CNRS 6595, Technopôle de Château Gombert, 5, Rue Enrico Fermi, 13 453 Marseille Cedex 13, France
[b] CETHIL, UMR CNRS 5008, Bâtiment Sadi Carnot, 20 Avenue Albert Einstein, 69621 Villeurbanne Cedex, France

Received 19 March 2003

Abstract

This paper deals with an inverse problem that consists of the identification of multiple line heat sources placed in a homogeneous domain. In the inverse problem under investigation the location and strength of the line heat sources are unknown. The estimation procedure is based on the boundary element method. As the discrete problem is non-linear if the location of the line heat sources is unknown, an iterative procedure has to be applied to find out the location of the sources. The proposed approach has been tested for steady and transient experiments. In the present study we propose an original approach to solve the steady problem. As in the steady heat conduction case we have a limited number of unknown for each source, a "parameter estimation" approach can be applied to estimate the sources. Using the techniques of parameter estimation, we can also estimate the confidence interval of the estimated locations, which permits to design an optimal experiment. We intend to present some numerical and experimental 2D results.

1. Introduction

In the last few years, the inverse heat conduction problem (IHCP) has been the subject of a lot of works in various fields of research. Domains such as unknown boundary conditions reconstruction or parameters identification have been widely investigated. Paradoxically, the bibliography on heat source term estimation in the fundamental equation of the heat transfers is not numerous. As this problem requires a lot of information (measurements) to be solved properly, most of the works on this subject are restricted to point heat sources estimation. However, some authors [1,2] present some methods to solve the general problem of an unknown general heat generation, but they propose only computational investigations.

The first works on point heat sources estimation have been proposed by Huang and Özisik [3] and Neto and Özisik [4–6] in 1992 and 1993. These works are based on the conjugate gradient method coupled with the finite element method (FEM) in transient heat conduction. The proposed methods have been applied to the strength estimation of one or two sources in the 1D and 2D cases when the location of the sources is known. In [5], the authors present a method to cope with both location and strength estimation for one source in a 1D geometry. More recently, Yang [7–9] used the FEM and the finite difference method to obtain a linear model for strength estimation when the location of the point heat sources is known. Compare to the conjugate gradient method previously described, the method developed by Yang permits to avoid the iterative calculations, which are inherent in the gradient methods. Nevertheless, the method is applied to a maximum of two sources and can not be use when the location of the sources is unknown. In the steady case, Karami and Hematiyan [10] propose the boundary element method (BEM) for strength or location estimation of multiple point heat sources in the 2D case. This method does not permit to estimate simultaneously the strength and the location of the heat sources but only one of these two variables, the other being known.

* Corresponding author. Tel.: +33-4-91-10-68-86; fax: +33-4-91-10-69-69.
E-mail addresses: christophe.leniliot@polytech.univ-mrs.fr (C. Le Niliot), lefevre@genserver.insa-lyon.fr (F. Lefèvre).

0017-9310/$ - see front matter © 2003 Elsevier Ltd. All rights reserved.
doi:10.1016/j.ijheatmasstransfer.2003.08.011

Nomenclature

$\mathbf{C}$, $\mathbf{G}$, $\mathbf{H}$, $\mathbf{I}$, $\mathbf{A_1}$	matrices
B_1	vector
d	distance
g	source strength ($\mathrm{W\,m^{-1}}$)
h	heat transfer coefficient ($\mathrm{W\,m^{-2}\,K^{-1}}$)
J	cost function
K	number of point sources
k	thermal conductivity ($\mathrm{W\,m^{-1}\,K^{-1}}$)
M	number of measurements
N	number of boundary elements
N'	number of internal points
P	heat flux vector
r	correlation coefficient
S	strength vector
T	temperature vector
x, y, z	Cartesian co-ordinates
$\mathbf{X}$	sensitivity matrix
Y	measurements vector

Subscripts

cal	direct calculation result
mes	measure
∞	ambient conditions
k	heat source index

Superscripts

$\wedge$	least squares solution
$\sim$	approximated heat source contribution
$'$	internal points
$*$	regular sensitivity coefficient

Greek symbols

β	parameters vector
ε	measurements error vector
λ	thermal conductivity ($\mathrm{W\,m^{-1}\,K^{-1}}$)
Θ	heat sources contribution vector
φ	heat flux ($\mathrm{W\,m^{-2}}$)
θ	temperature (°C)
Γ	boundary
σ	standard deviation
η	measurements model vector
ξ	sensitivity coefficient
v	number of freedom degrees

All the papers previously mentioned are purely numerical investigations. As inverse problems are very sensitive to measurements errors, they have to be tested with experimental data. It is only in dealing with real data that one is able to get the bugs out of the system and understand what will and will not work. In 2001, we have presented the results of a steady experiment for multiple sources in 2D [12]. This method, based on BEM, is available for multiple sources for both location and strength estimation. In these 2D applications, an infrared scanner is used to obtain the boundary measurements and some internal measurements are given by thermocouples. Recently, Abou Khachfe and Jarny [11] have proposed the FEM associated to a conjugate gradient algorithm to cope with the location and strength identification of multiple point heat sources. This method has been tested on a 2D experiment, which uses only boundary measurements given by thermocouples. This method gives good results for the identification of two sources, but the author concludes by highlighting the interest of an infrared scanner to identify more sources.

In all the previous works, the methods are restricted to the estimation of one or two point heat sources and the inverse problem of location estimation is rarely considered. In 2002 [13], we have proposed a numerical method to estimate the location and the strength of multiple static heat sources in transient heat conduction. This method can also cope with the estimation of a moving source in 2D or 3D domains. In a recent work [14], we have tested our method on 2D experiments for the case of multiple static heat sources and for the case of a moving heat source. 3D applications are difficult to perform due to experimental problems to produce a controlled point source with a significant strength.

BEM is well adapted to point heat source treatment because it does not require any refined mesh around the point heat source as in FEM. Indeed, for BEM taking into account different locations for a point heat source in 2D problems leads to a log function calculation of the co-ordinates in steady case and incomplete gamma function calculation of the co-ordinates in transient case.

As in steady heat conduction the number of unknown parameters for each source is restricted to one strength and two (in 2D) or three (in 3D) co-ordinates, a parameter estimation approach can be applied to identify the sources. As it was previously mentioned, inverse problems are very sensitive to measurements errors; this is the reason why it is important to test the identification methods with experimental data and of course to give an estimation of the confidence interval surrounding the result of the inversion. This aspect of the problem is never discussed in the literature dealing with heat source estimation even in our contribution [12].

In our previous work [12] the strength is obtained with a linear function estimation procedure using an

inverse formulation of BEM. The locations are obtained using an iterative procedure once the strengths are known. In [12] the scope of the paper was to show that we could estimate both the strength and the location of multiple sources. The proposed numerical approach didn't permit us to estimate the confidence interval around each sources knowing the noise in the measurements. In this paper, we propose an original method, which is based on a parameter estimation procedure. In this case, BEM is used to build the direct model of the measurements. This new procedure permits to estimate the confidence interval of the estimated locations and strengths, particularly to determine if an accurate estimation is possible or not.

This paper is divided in two parts. The first one describes in details the parameter estimation approach of Beck and Arnold [15] applied to our problem of point heat source estimation and the second one presents some numerical results.

2. The "parameter estimation" approach

In this part, we present the parameter estimation procedure for point heat sources identification in steady heat conduction. The method used here is based on the work of Beck and Arnold [15]. The heat source term is not strictly a parameter of the steady heat conduction equation but rather an input of the system. Without any information on the form of the heat source function, the inverse problem can not be treated as a parameter estimation procedure but as a function estimation procedure. Nevertheless, in the case of point heat sources, this approach is possible because the number of unknowns is known and limited to one strength and two (in 2D) or three (in 3D) co-ordinates for each source.

If we follow the parameter estimation approach recommended by most of the authors, we have to produce a mathematical model of our measurements. BEM permits to build this mathematical model.

2.1. The mathematical model using BEM

Let us introduce briefly the BEM. Considering point M, in domain Ω of boundary Γ, integrating twice the linear steady heat transfer equation weighted by a fundamental solution T^*, leads to the boundary integral equation (BIE) for the linear stationary heat conduction

$$\theta_M + \int_\Gamma \theta_q^* \,\mathrm{d}\Gamma = \int_\Gamma \frac{\varphi}{\lambda} T^* \,\mathrm{d}\Gamma + \int_\Omega \frac{g}{\lambda} T^* \,\mathrm{d}\Omega \tag{1}$$

Here φ is the heat flux, T^* the fundamental solution, q^* the normal derivative of T^* and c a coefficient which depends on the position of M. Namely $c = 1$ if M is in Ω and $c < 1$ if M is on Γ (e.g. $c = 0.5$ if Γ is smooth at M). Fundamental solution T^* is a space dependent Green function, which allows local measurements (internal points) and singularities as point heat sources. Function T^* used to obtain Eq. (1) is a solution of

$$\Delta T^* + \delta_M = 0 \tag{2}$$

where δ_M is the Dirac function at point M in domain Ω. Here T^* is a Green function that represents the response to a point heat source in an infinite domain. Thus, T^* can be written

$$\text{in 2D,} \quad T^* = \frac{1}{2\pi} \ln\left(\frac{1}{d}\right) \quad \text{and} \quad \text{in 3D,} \quad T^* = \frac{1}{4\pi}\frac{1}{d} \tag{3}$$

where, in both cases, d is the distance between the current node and the point M of domain Ω. BIE (1) lets appear a volume integral relative to heat source term g. In order to transform this volume integral in a discrete form without a complete domain mesh let us consider g as a set of K point heat sources [12]. By applying this last property, the heat source term in BIE (1) can be written

$$\int_\Omega \frac{g}{\lambda} T^* \,\mathrm{d}\Omega = \sum_{k=1}^{K} \frac{g_k}{\lambda} T^*(d_{M,k}) \tag{4}$$

Here g_k is the algebraic strength of source k and $T^*(d_{M,k})$ is function T^* calculated for the distance from point M to source k. This last equation explain why BEM is well adapted to cope with point heat sources: we transform a singular point heat source in a discrete sum function of the distances $d_{M,k}$.

To perform a parameter estimation procedure, we have to obtain a mathematical model of the measurements. This model can be built using the boundary integral discrete formulation for the N boundary elements and the N' internal points. If we use a constant approximation, which means that heat flux and temperature are constant over a boundary element we have the following matrix expression:

$$\begin{bmatrix} 0 \\ T' \end{bmatrix} + \begin{bmatrix} \mathbf{H} \\ \mathbf{H}' \end{bmatrix} T - \begin{bmatrix} \mathbf{G} \\ \mathbf{G}' \end{bmatrix} P = \begin{bmatrix} \mathbf{I} \\ \mathbf{I}' \end{bmatrix} S \tag{5}$$

In this last equation, T' is the vector of the N' internal temperatures, $T(P)$ is the vector of the N boundary temperatures (heat flux) and S is the vector of the K sources strengths. Matrices $\mathbf{H}$ and $\mathbf{G}$ of dimension (N,N) depends on the boundary mesh only. $\mathbf{H}'$ and $\mathbf{G}'$ of dimension (N',N) depends on the internal points locations. Matrices $\mathbf{I}$ and $\mathbf{I}'$ depends on the distance d between the point heat source and the concerned boundary element (internal point). This function is a log function in 2D and a $1/d$ function in 3D (see (3)).

Let assume that both temperature and heat flux are measured on the boundary. The heat flux is obtained from the temperature with a known heat transfer coefficient.

This type of boundary condition, called the double specified boundary condition, is necessary to solve the inverse problem of heat sources estimation if we don't have internal measurements. The double specified boundary condition is not necessary on the entire boundary and we can have a simple boundary condition on a part of the boundary.

Nevertheless, considering the boundary conditions, the inverse problem of point heat sources estimation requires measurements, which should be at least equal to the number of unknowns. It is therefore necessary to obtain these measurements from the boundary or from internal measurements.

Let us assume for the numerical development that the heat transfer coefficient h is constant along the boundary, we obtain

$$\varphi(i) = h(\theta(i) - \theta_\infty) \tag{6}$$

In this last equation, θ_∞ is the ambient temperature, $\varphi(i)$ and $\theta(i)$ are, respectively, the heat flux and the temperature for boundary element Γ_i. Let us introduce (6) in (5), we obtain

$$\begin{bmatrix} 0 \\ T' \end{bmatrix} + \begin{bmatrix} \mathbf{H} \\ \mathbf{H}' \end{bmatrix} T = h \begin{bmatrix} \mathbf{G} \\ \mathbf{G}' \end{bmatrix} T - h \begin{bmatrix} \mathbf{G} \\ \mathbf{G}' \end{bmatrix} T_\infty + \begin{bmatrix} \mathbf{I} \\ \mathbf{I}' \end{bmatrix} S \tag{7}$$

We assemble together the coefficient of the boundary and internal temperatures into a matrix $\mathbf{A}$ and we introduce vector B, which depends on the ambient conditions. We obtain the following expression for $\mathbf{A}$ and B:

$$\mathbf{A} = \begin{bmatrix} \begin{bmatrix} \mathbf{H} - h\mathbf{G} \\ \mathbf{H}' - h\mathbf{G}' \end{bmatrix} & 0 \\ 0 & 1 \end{bmatrix} \quad \text{and} \quad B = h \begin{bmatrix} \mathbf{G} \\ \mathbf{G}' \end{bmatrix} T_\infty \tag{8}$$

Introducing $\mathbf{A}$ and B in (7), we obtain

$$\mathbf{A} \begin{bmatrix} T \\ T' \end{bmatrix} = \begin{bmatrix} \mathbf{I} \\ \mathbf{I}' \end{bmatrix} S - B \tag{9}$$

$\mathbf{A}$ is a square matrix of dimension $(N + N', N + N')$. The mathematical model of the measurements η can also be written

$$\eta = \begin{bmatrix} T \\ T' \end{bmatrix} = \mathbf{A}^{-1} \left\{ \begin{bmatrix} \mathbf{I} \\ \mathbf{I}' \end{bmatrix} S - B \right\} \tag{10}$$

Using this approach we can obtain an estimation of the error on the identified locations and strength. This general formulation is given for N boundary elements and N' internal points. In the following examples we do not use any thermocouple ($N' = 0$) and we use only some superficial temperature measurements obtained using infrared thermography. In the following the total number of measurements is M.

In our steady state estimation procedure described in [12], we introduced two vectors: $\widehat{\boldsymbol{\Theta}}$ and $\widetilde{\boldsymbol{\Theta}}$. These vectors are built from a discrete form of the boundary integral equation (see [12]). $\widehat{\boldsymbol{\Theta}}$ is the vector of the boundary variables contribution and $\widetilde{\boldsymbol{\Theta}}$ the vector of the heat sources contribution, which depends of the sources strength and location. With $\widetilde{\boldsymbol{\Theta}}$, we have a mathematical model of the heat source term that we can compare to $\widehat{\boldsymbol{\Theta}}$, which is a linear combination of the measurements. In [12], the problem is solved in two steps: a linear function estimation of the strength and an iterative procedure to estimate the location. Here we will use vector $\eta(\beta)$ to estimate the strength and the location in the same procedure.

2.2. Error on the estimated parameters

In the first part we have presented the model $\eta(\beta)$ of the measurements contained in a vector Y. If there is no measurement errors on the temperatures contained in vector Y and no biased error in the model we have $Y = \eta(\beta)$ for the exact location and strength contained in parameters vector β. In 2D, considering co-ordinates x_l, y_l, and strength g_l of the sources $(0 \leqslant l \leqslant K)$ as some parameters assembled in vector β, we can obtain an estimation of the error on the estimated location and strengths. The method is the statistical approach recommended by Beck and Arnold [15]. We describe in the following paragraphs the procedure applied in our case.

2.2.1. Definition of the cost function

The model is a non-linear function of the co-ordinates but a linear function of the strength. This property led us to separate the two estimations: a non-linear iterative procedure for the co-ordinates and a linear estimation of the strength. The detailed approach is given in [12] with some experimental examples.

In order to take into account the influence of an estimated parameter on the others, we consider here a unique cost function for all the parameters. To perform this non-linear parameters estimation we build a quadratic cost function and we apply a non-linear least square procedure to obtain an estimation $\hat{\beta}$ of β. The cost function to be minimised is

$$J(\beta) = \sum_{i=1}^{M} (Y_i - \eta_i(\beta))^2 \tag{11}$$

In this last equation, subscript i make reference to the ith measurement. Minimising J with respect to parameters β_j leads to find

$$\frac{\partial J}{\partial \beta_j} = 0 \Rightarrow \sum_{i=1}^{M} \frac{\partial \eta_i(\beta)}{\partial \beta_j} (Y_i - \eta_i(\beta)) = 0 \quad (\forall j) \tag{12}$$

Introducing sensitivity coefficient $X_{i,j}$ which correspond to the first derivative of the model for the ith measurement with respect of parameter β_j, we obtain

$$X_{i,j} = \frac{\partial \eta_i(\beta)}{\partial \beta_j} \tag{13}$$

Let us define sensitivity matrix $\mathbf{X}$ of component $X_{i,j}$. Using sensitivity matrix X, we can write a matrix form of equation (12) and we obtain the following system of equations:

$$\mathbf{X}^{\mathrm{T}}(Y-\eta)=0 \tag{14}$$

As we have a non-linear estimation, the solution is obtained through an iterative process with a first order development of the errors. For measurement i at iteration $n+1$ we obtain

$$\eta_i(\hat{\beta}^{n+1}) \approx \eta_i(\hat{\beta}^n) + \sum_j (\hat{\beta}_j^{n+1} - \hat{\beta}_j^n) X_j(i,\beta)|_{\beta=\hat{\beta}^n} \tag{15}$$

This last equation can be written in a matrix form

$$\eta^{n+1} = \eta^n + \mathbf{X}^n(\hat{\beta}^{n+1} - \hat{\beta}^n) \tag{16}$$

Around the solution we can write that system of equations (14) is correct. If we substitute η^{n+1} by its first development, we obtain a connection between the estimated parameters at iterations n and $n+1$. At least estimated vector β at iteration $n+1$ is obtained solving the following system of linear equations:

$$\hat{\beta}^{n+1} = \hat{\beta}^n + (\mathbf{X}^{n^{\mathrm{T}}}\mathbf{X}^n)^{-1}\mathbf{X}^{n^{\mathrm{T}}}(Y-\eta^n) \tag{17}$$

The estimated vector β^{n+1} can be connected using the sensitivity matrix to the estimated vector obtained using the cost function presented at Eq. (11) and described in details in [12]. Let us note that vector β contains the location and strength of the point heat sources.

2.2.2. Statistic considerations

Measurements contained in vector Y are generally not exact. The measurement errors produce on the estimated vector $\hat{\beta}$ some errors, amplified by the ill-posed character of the inverse problem. We assume that the measurements errors ε_i are: uncorrelated, Gaussian with an average $E(\varepsilon)$ equal to 0 and a constant variance σ^2. These statistical properties are applied to internal and superficial measurements. Thus, all the measured temperatures $\widetilde{Y}_i$ on each element Γ_i corresponding to the exact data η_i are given according to the following equation:

$$\widetilde{Y}_i = \eta_i(\beta) + \varepsilon_i \tag{18}$$

We try to estimate the errors introduced by the measurement errors on the estimated parameters. Let us assume that the values, results of the iterative process are close to the optimal values and that they are solutions of

$$\mathbf{X}^{\mathrm{T}}|_{\beta=\hat{\beta}}(\widetilde{Y} - \eta(\hat{\beta})) = 0 \tag{19}$$

If we develop η around the solution we obtain

$$\eta(\hat{\beta}) = \eta(\beta) + \mathbf{X}|_{\beta}(\hat{\beta} - \beta) \tag{20}$$

Using Eq. (20) in (19), we obtain a relation between the real parameters and the estimated ones and we have

$$\hat{\beta} = \beta + (\mathbf{X}^{\mathrm{T}}\mathbf{X})^{-1}\mathbf{X}^{\mathrm{T}}\varepsilon \tag{21}$$

Here vector ε is the vector of the measurement error. Using this last equation with the assumptions on the statistical properties of the measurement errors we can obtain the properties of the estimated vector $\hat{\beta}$, these properties are also given in [15]. The final results are

$$\begin{aligned} E(\hat{\beta}) &= \beta + E((\mathbf{X}^{\mathrm{T}}\mathbf{X})^{-1}\mathbf{X}^{\mathrm{T}}\varepsilon) \\ &= \beta + (\mathbf{X}^{\mathrm{T}}\mathbf{X})^{-1}\mathbf{X}^{\mathrm{T}}E(\varepsilon) = \beta \end{aligned} \tag{22}$$

and

$$\mathbf{V}(\hat{\beta}) = \sigma^2(\mathbf{X}^{\mathrm{T}}\mathbf{X})^{-1} \tag{23}$$

It has to be noticed that the variance-covariance matrices are calculated using a linear approximation around the solution. This linear assumption will be justified only if we are very close to the solution. As a result the diagonal terms of matrix (23) are the variance of each parameter and we can obtain the standard deviation using the square root of these variances.

We can estimate the correlation between all the parameters by calculating the correlation coefficient $r_{i,j}$ between estimated parameters $\hat{\beta}_i$ and $\hat{\beta}_j$. If we note V the variance, we have

$$r_{i,j}^2 = \frac{V_{i,j}^2}{V_{j,j}V_{i,i}} \tag{24}$$

The value of $r_{i,j}$ is in the range -1 and 1 and we consider that the parameters are highly correlated when $|r_{i,j}| \geqslant 0.9$.

2.3. Confidence region and interval

If we perform p experiments (p estimations) we find $100(1-\alpha)\%$ of these estimations inside a confidence region at level $(1-\alpha)$ centred on the value $\beta = E(\hat{\beta})$. If we assume a Gaussian distribution around their mean value, such a confidence region is represented by a hyper ellipsoid which equation is

$$(\hat{\beta}-\beta)^{\mathrm{T}}\mathbf{V}^{-1}(\beta-\hat{\beta}) = \chi^2_{1-\alpha}(\nu) \tag{25}$$

Here $\chi^2_{1-\alpha}(\nu)$ is the calculated value of χ^2 for ν freedom degrees and a probability level equal to $1-\alpha$ [16]. The exact value of each parameter is in the range

$$\hat{\beta}_i - \sigma_i\sqrt{\chi^2_{1-\alpha}(\nu)} \leqslant \beta_i \leqslant \hat{\beta}_i + \sigma_i\sqrt{\chi^2_{1-\alpha}(\nu)} \tag{26}$$

In the following we present the confidence region with a confidence interval equal to 99%.

3. Numerical examples of the parameter estimation method for point heat source estimation

In this part, we propose some numerical results obtained for the estimation of one to four heat sources in a 2D system. The numerical simulation is similar to the experimental one presented in [12]. It concerns a long cement bar of section 50×50 mm^2 crossed in its longest dimension by multiple line heat sources. A cross section of the bar is shown in Fig. 1.

The measurements necessary to solve the inverse problem are some temperatures calculated by a direct computation. The temperature field is obtained considering a constant heat transfer coefficient $h = 10$ W m^{-2} K^{-1} on the four sides, an ambient temperature θ_∞ equal to 0 °C. A thermal conductivity λ equal to 1 W m^{-1} K^{-1} is adopted which is a value close to that of cement (0.85 W m^{-1} K^{-1}). The computational domain is discretised into 100 linear elements ($N = 100$), 25 per side of the square bar, which is sufficient to solve correctly the direct problem. In order to test the sensitivity of the method to measurement errors, the numerical temperature are disrupted by an additional Gaussian error of zero mean value and standard deviation σ.

In all the presented examples we have $N = 100$ elements and we try to avoid the internal sensors (thermocouples), nevertheless we present an example using two and three ($N' = 3$) thermocouples. The measurements are the temperature at the N boundary nodes, thus we have the number of measurements $M = N = 100$.

3.1. Analysis of the sensitivity coefficients

We present below a study of the sensitivity coefficients to the location and the strength of the point heat sources. The sensitivity coefficients are obtained from Eq. (13). The aim of this study is to evaluate the feasibility of the inversion according to the number of heat sources and temperature measurements. In parameter estimation procedures some authors prefer to use the normalized sensitivity coefficient X^* rather than the regular sensitivity coefficient X (cf. Eq. (13)). The normalized sensitivity coefficient is defined by

$$X^*_{i,j} = \hat{\beta}_j \frac{\partial \eta_i(\beta)}{\partial \beta_j} \tag{27}$$

Here sensitivity coefficient $X^*_{i,j}$ which corresponds to the first derivative of the model for the ith measurement with respect to parameter β_j multiplied by an estimation $\hat{\beta}_j$ of parameter β_j. Normalized sensitivity coefficient is more convenient to compare sensitivity coefficient for different nature of parameters: here the strength and the location of the heat sources. It is impossible to present some normalized sensitivity coefficients related to the coordinates of the source, x or y, because they are function of the chosen co-ordinate system. Nevertheless we can present some normalized sensitivity coefficients calculated with the distance $d_{M,k}$ from the source to the boundary node, this distance is used to calculate function T^* (cf. Eq. (3)). For boundary node i and source k at location (x_k, y_k) of strength g_k we have three sensitivity coefficients X^*

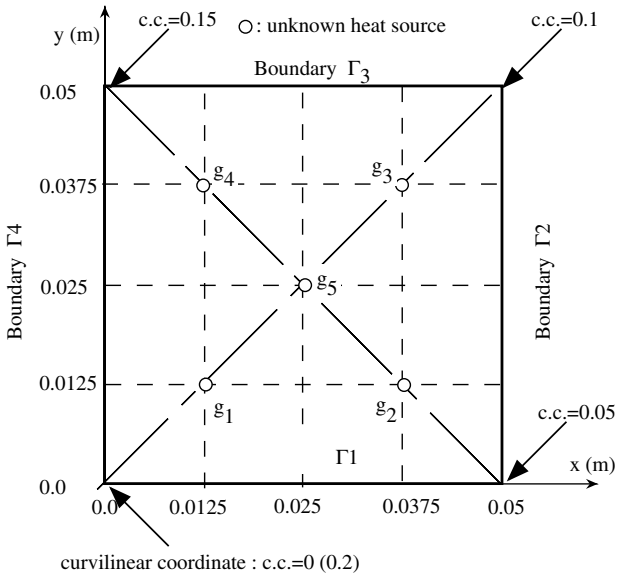

Fig. 1. Scheme of the studied 2D section.

$$d_{i,k}\frac{\partial \eta_i(\beta)}{\partial x_k}$$

for the sensitivity to a variation of the x co-ordinate

$$d_{i,k}\frac{\partial \eta_i(\beta)}{\partial y_k}$$

for the sensitivity to a variation of the y co-ordinate

$$g_k\frac{\partial \eta_i(\beta)}{\partial g_k}$$

for the sensitivity to a variation of the strength (28)

For the normalized sensitivity coefficients obtained for the co-ordinates, we use a displacement of 1 mm on x or y and we multiply the result by the distance d, also in mm. We present in Figs. 2 and 3 the sensitivity coefficients to the co-ordinates of different sources activated with a strength of 10 $W\,m^{-1}$ versus the curvilinear co-ordinate. On each figure, we present two cases related to sources g_1 or g_5, the other sources being not activated. Considering the geometry (see Fig. 1) the other cases corresponding to sources g_2, g_3 and g_4 can be deducted from g_1. Mainly for our system the sensitivity coefficients have a sufficient magnitude in order to estimate the location if the temperature is measured on the four boundaries.

In Figs. 4 and 5 we present the normalized sensitivity coefficients for a displacement of x and y. As we can see in these two figures, coefficients X_x^* and X_y^* are not correlated, and it will be possible to estimate both x and y for the two sources with our measurements. In the next paragraph we will examine the possibility to estimate both g_1 and g_5 in the same test.

The influence of the strength to the sensitivity coefficients to the co-ordinate x is shown in Fig. 6 for source g_5 activated with two different strengths of 10 or 40 $W\,m^{-1}$. As the sensitivity coefficients are linearly variable with the strength, they are four times higher for a strength equal to 40 $W\,m^{-1}$ than for a strength equal to 10 $W\,m^{-1}$.

In Fig. 7, we present the sensitivity coefficients to the strength of the sources as a function of the curvilinear co-ordinate. The sensitivity coefficients for g_5 are symmetrical on each boundary, because g_5 is located in the center of the system. This is not the case for g_1 for which the sensitivity is higher on some parts of the boundary due to the lower distance from the source to the scanned boundary. As a result the strength and location identification with only infrared data is possible: a lack of sensitivity on a boundary is balanced by a higher sensitivity elsewhere. The second conclusion is that it is possible to estimate both strength and location of a single source, for example g_5. If we examine Figs. 6 and 7, it is obvious that the sensitivity coefficients for the location and the strength are not correlated. This is not the case when we have several sources activated at the same time as presented in the next paragraph.

3.2. Confidence interval for the experimental geometry

The numerical examples proposed in this part aim to illustrate the sensitivity coefficient study described previously. In order to simulate measurements errors, an additional Gaussian error of zero mean value and standard deviation σ is added to the temperature field

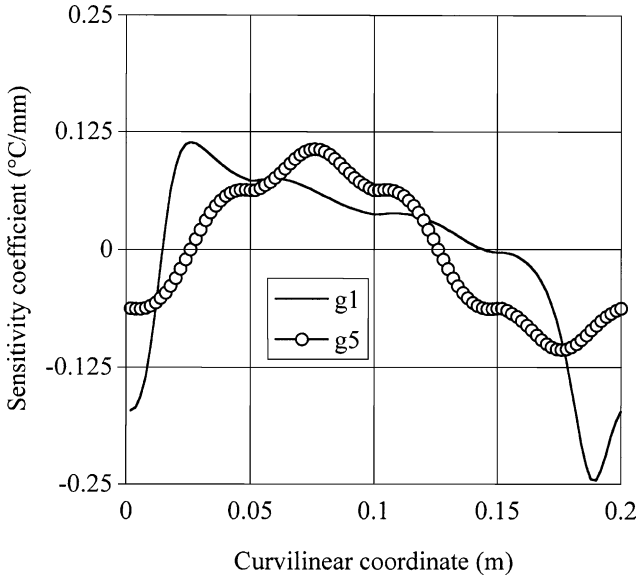

Fig. 2. Sensitivity coefficient to x along the scanned boundaries for different sources activated with a strength of 10 $W\,m^{-1}$.

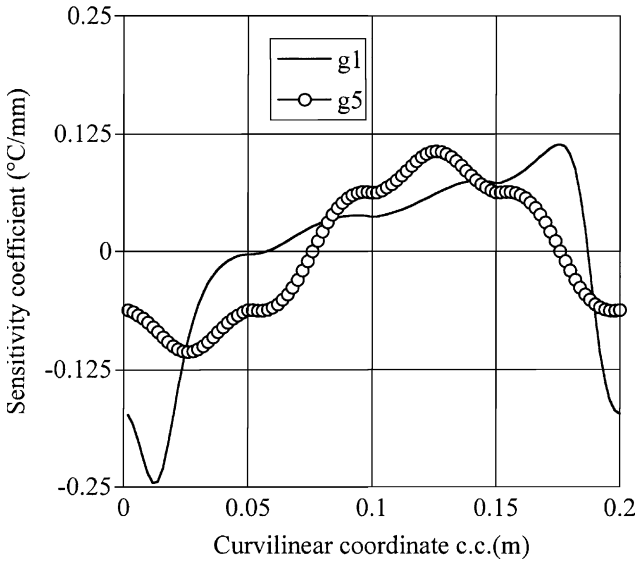

Fig. 3. Sensitivity coefficient to y along the scanned boundaries for different sources activated with a strength of 10 W m^{-1}.

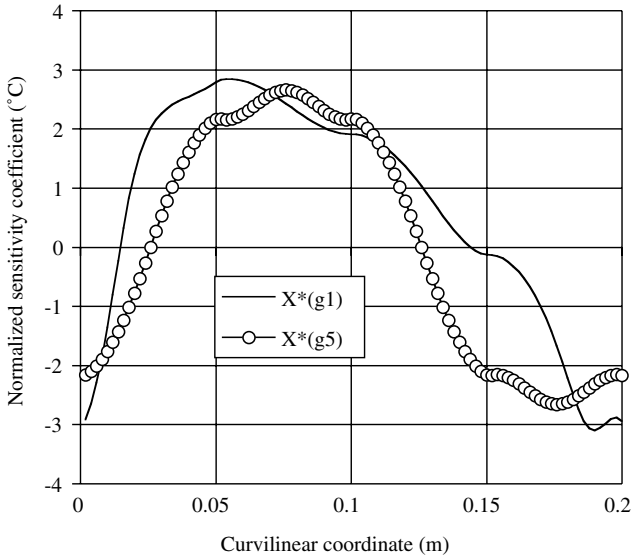

Fig. 4. Normalized sensitivity coefficient to x along the scanned boundaries for different sources activated with a strength of 10 W m^{-1}.

obtained from a direct calculation with a confidence interval at 99% equal to $\pm 2.576 \times \sigma$.

3.2.1. Numerical simulation from the experimental case

In the first example, four sources g_1, g_2, g_3 and g_4 are activated with, respectively, 10, 20, 30 and 40 W m^{-1}. This example is a numerical simulation of an experimental case presented in [12]. The results of the experimental estimation are given in Table 1. In this table we find the errors between the estimated parameters and the real parameters. The results of this experiment are good but considering the approach presented in [12] we cannot give any confidence interval.

In order to compare the parameter estimation approach results to the experimental results given in [12], we propose some numerical experiments in the same conditions. In this virtual experiment we find the four sources g_1, g_2, g_3 and g_4 activated with, respectively, 10, 20, 30 and 40 W m^{-1}. We present some results with two levels of additional noise to the temperature field ob-

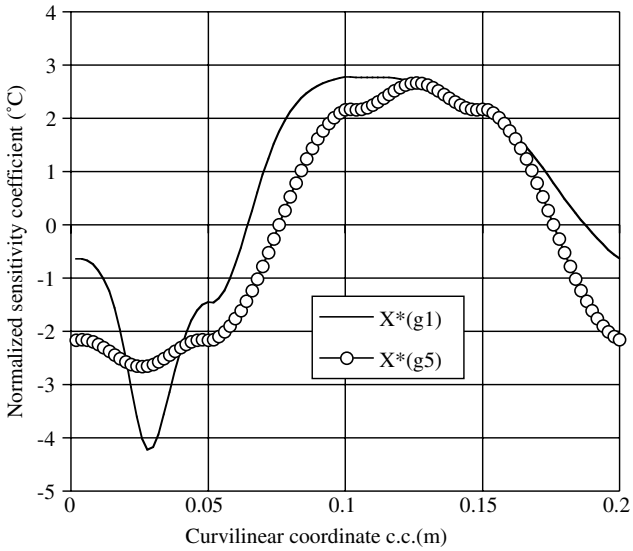

Fig. 5. Normalized sensitivity coefficient to y along the scanned boundaries for different sources activated with a strength of 10 W m^{-1}.

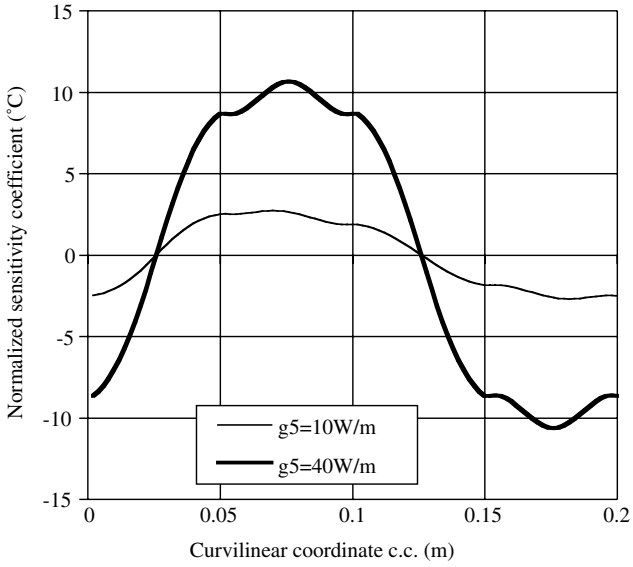

Fig. 6. Normalized sensitivity coefficient to x variation for g_5 activated with two different strengths versus curvilinear co-ordinate.

tained with the direct problem: $\sigma = 0.1$ °C for good quality measurements and $\sigma = 0.5$ °C for poor quality measurements. An example of the error and the temperature field obtained from a direct calculation is presented in Fig. 8 versus the curvilinear co-ordinate. Compared to the average boundary temperature (around 50 °C) we have a relative error of 0.5% for $\sigma = 0.1$ °C and 2.6% for $\sigma = 0.5$ °C.

The results of the 100 parameter estimations are assembled in a 3D graph (see Fig. 9). The base is the plan (X, Y) and the vertical axe represents the strength of the estimated source. As it could be predicted, the results are much more stable using good quality measurements (Fig. 9a) than with poor quality measurements (Fig. 9b). The mean values and the standard deviation for each parameter are given in Table 2 ($\sigma = 0.1$ °C) for good quality measurements and in Table 3 ($\sigma = 0.5$ °C) for poor quality data. These results are very similar to the experimental results given in Table 1. In Fig. 9, we can see that if a location is found "deeper" in the bar, its

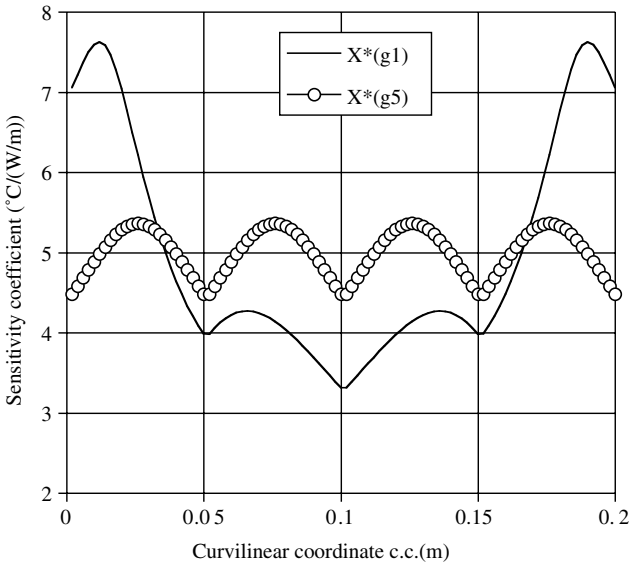

Fig. 7. Normalized sensitivity coefficient to source strength for sources g_1 (10 W m^{-1}) and g_5 (10 W m^{-1}) versus curvilinear co-ordinate.

Table 1
Results of an estimation on a live experiment involving four sources ($g_1 - g_4$), extract from Le Niliot and Lefèvre [12]

Source	Strength g (W m^{-1})	Error Δg (W m^{-1})	Distance: estimated-real (mm)	Error on x co-ordinate (mm)	Error on y co-ordinate (mm)
g_1	10	0.0	3.5	−0.6	−3.5
g_2	20	2.3	1.9	1.9	0.3
g_3	30	−3.5	1.4	0.1	1.4
g_4	40	−1.4	0.4	−0.4	−0.1

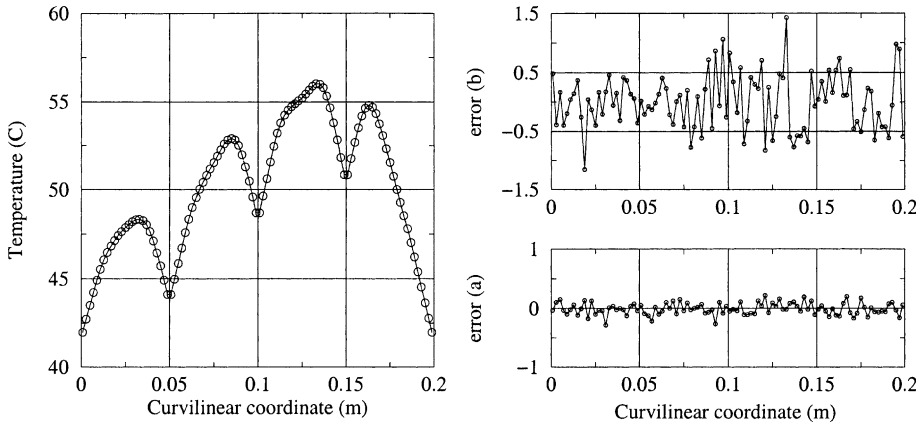

Fig. 8. Temperature field and corresponding measurement error for the case presented in Fig. 9; error: (a) ($\sigma = 0.1$ °C) and (b) ($\sigma = 0.5$ °C).

strength is over estimated. This is the case for g_1 which location is estimated nearly at the centre (see Fig. 9b) with a strength of 46 W m^{-1} instead of 10 W m^{-1}. We can see also the correlation between the level of the strength and the quality of the location estimation. As we can see in Tables 2 and 3, as the strength increases

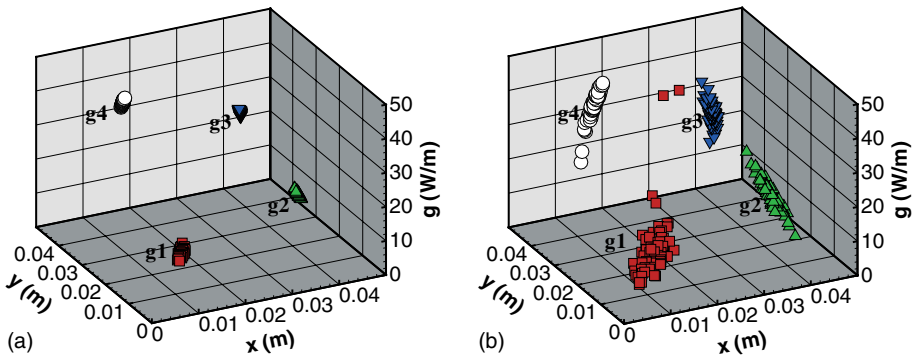

Fig. 9. Location estimation results for four sources g_1, g_2, g_3 and g_4 activated with respectively 10, 20 30 and 40 W m^{-1}. Results for: (a) $\sigma = 0.1$ °C and (b) $\sigma = 0.5$ °C.

Table 2
Results of an estimation on a virtual experiment for four sources g_1, g_2, g_3 and g_4 activated with, respectively, 10, 20, 30 and 40 W m^{-1}, results obtained with $\sigma = 0.5$ °C and 100 estimation results

Source	Mean value of the estimated strength, g (W m^{-1})	Standard deviation on strength, g (W m^{-1})	Mean value of estimated co-ordinate (mm)		Standard deviation on the estimated co-ordinate (mm)	
			x	y	σ_x	σ_y
g_1	10.1	0.5	12.6	12.6	2.9	2.9
g_2	19.9	0.5	37.5	12.5	0.2	0.2
g_3	29.9	0.5	37.5	37.5	0.1	0.2
g_4	40.1	0.5	12.5	37.5	0.1	0.1

Table 3
Results of an estimation on a virtual experiment for four sources g_1, g_2, g_3 and g_4 activated with, respectively, 10, 20, 30 and 40 W m^{-1}, results obtained with $\sigma = 0.5$ °C and 100 estimation results

Source	Mean value of the estimated strength, g (W m^{-1})	Standard deviation on strength g, (W m^{-1})	Mean value of estimated co-ordinate (mm)		Standard deviation on the estimated co-ordinate (mm)	
			x	y	σ_x	σ_y
g_1	11.1	6.2	12.6	12.6	2.9	2.9
g_2	19.7	3.6	37.7	12.4	1.3	1.3
g_3	29.7	3.5	37.6	37.6	0.9	0.9
g_4	39.4	4.1	12.4	37.6	0.7	0.7

the standard deviation of the co-ordinates decreases. This result confirms the sensitivity analysis presented in Fig. 6, where the sensitivity to the location increases linearly with the strength of the source. As a result the other sources are found near the boundary with a strength lower than expected. This 3D representation does not permit to present clearly all the results obtained, particularly the confidence interval.

The results of the location estimation are presented in an other manner in Fig. 10. The estimated locations obtained from 100 numerical simulations where the measurements are disrupted with 100 different Gaussian distributions are presented with their confidence area projected onto the plane of the co-ordinates. Each confidence area is given with a confidence interval equal to 99% and 12 freedom degrees (3 per source). The additional error for the temperature field is different for each one of the 100 simulations. In Fig. 10(a) the Gaussian error has a standard deviation σ equal to 0.1 °C and in Fig. 10(b) σ is equal to 0.5 °C.

The estimated co-ordinates with the 100 simulations are located within the confidence ellipse. As it was

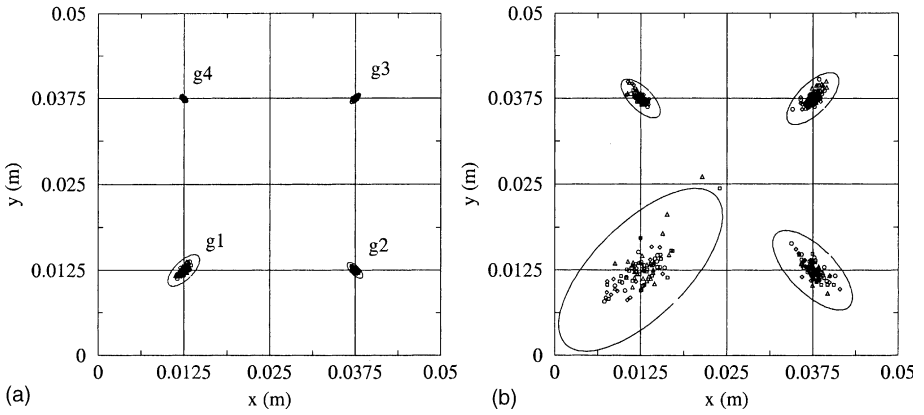

Fig. 10. Location estimation results for four sources g_1, g_2, g_3 and g_4 activated with respectively 10, 20 30 and 40 $W m^{-1}$. Results for (a) $\sigma = 0.1$ °C and (b) $\sigma = 0.5$ °C.

predictable from the sensitivity coefficients study, the confidence interval is high when the strength of the heat source is low (for g_1 with 10 $W m^{-1}$) and becomes smaller when the strength grows. For a standard deviation σ equal to 0.1 °C, which is a realistic error for infrared thermography, the results show that it is possible to estimate this configuration with a good precision. For a standard deviation σ equal to 0.5 °C, the estimation of g_1 becomes difficult, see also Table 3, but this last example corresponds to very poor quality measurements. These results confirm the experimental results presented in [12] for a similar case (cf. Table 1).

3.2.2. Results obtained with less measurements

The second example is similar to the previous one. Four sources (g_1–g_4) are activated with the same strength g equal to 25 $W m^{-1}$. In this case, we present the results of the estimation when the information to solve the inverse problem becomes smaller. In all the presented results, the standard deviation of the error added to the direct temperature field is equal to 0.1 °C.

The first result presented in Fig. 11 is obtained, as in the previous case, when both the temperature and the heat flux is known on the whole boundary. As we can see the results of the estimation are very good with an error lower than 1 mm for the co-ordinates.

In Fig. 12(a), we present the results of the location estimation when both the temperature and the heat flux are known on three faces (Γ_1, Γ_2 and Γ_3), the forth one (Γ_4) being submitted to a Fourier boundary condition with a heat transfer coefficient h equal to 10 $W m^{-2} K^{-1}$. In Fig. 12(b), the temperature and the heat flux are known on boundaries Γ_1 and Γ_3 when Γ_2 and Γ_4 are submitted to a Fourier boundary condition.

The confidence ellipses lose their shape compare to the precedent case. The variance on co-ordinate y be-

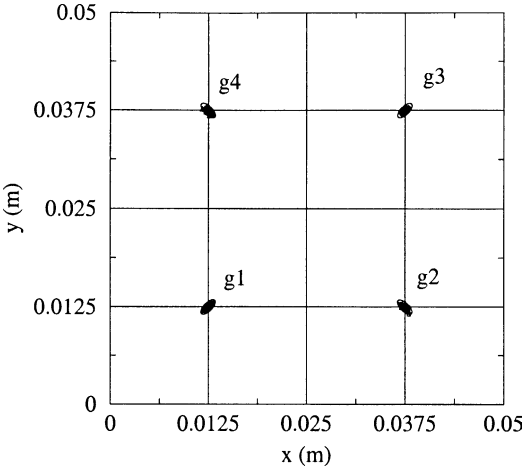

Fig. 11. Location estimation results for four sources g_1, g_2, g_3 and g_4 activated with the same strength equal to 25 $W m^{-1}$. The temperature and the heat flux are given on the whole boundary and $\sigma = 0.1$ °C.

comes more important for the sources situated near the face. For these sources we have a lack of information for y co-ordinates. This result can be explained regarding the sensitivity coefficient study presented before. Let us take for example Fig. 12(b), which is symmetrical. For g_1, the sensitivity coefficients to y and to the strength are linearly dependant on face Γ_1, where we get the information. This correlation between the co-ordinate y and the strength of source g_1 explains that the error on co-ordinate y and strength is much more important than for co-ordinate x. A large error on y co-ordinate is compensated by a large error on the strength as in the results presented in Fig. 9.

In the last example for this configuration, the temperature and the heat flux are known on two faces,

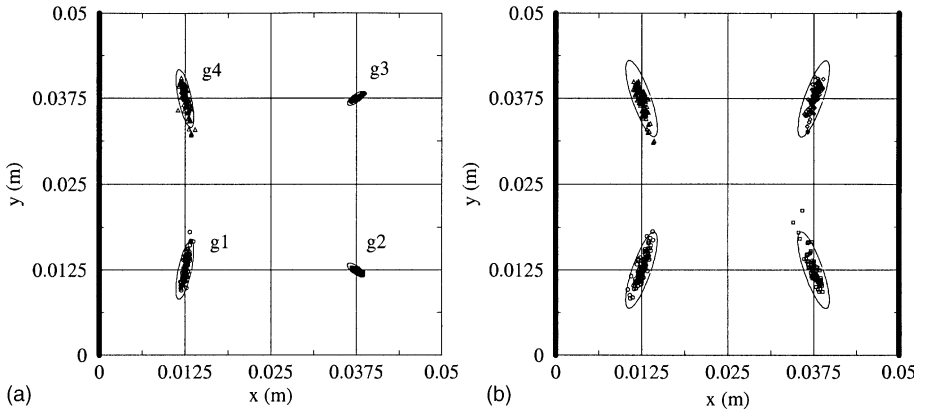

Fig. 12. Location estimation results for four sources g_1, g_2, g_3 and g_4 activated with the same strength equal to 25 W m^{-1}. Result for $\sigma = 0.1$ °C. Temperature and heat flux are given on: (a) Γ_1, Γ_2 and Γ_3 and (b) Γ_1 and Γ_3 only.

which are closed together (Γ_1 and Γ_2), the other boundaries (Γ_3 and Γ_4) being submitted to a Fourier boundary condition. For g_4, which is situated in the corner where there is a lack of information, the confidence ellipse is higher than the dimension of the square section. This source can not be estimated without additional information. We present in Fig. 13 the location estimation results when two or three thermocouples where used to solve the estimation problem.

These results show that a minimum of three sensitive sensors is necessary to estimate correctly g_4. With two temperature sensors, as it is shown in Fig. 13(a), for any location situated on a line between the two sensors we have a strength, which permits the model to fit the measurements. With three temperature sensors well located, an estimation of g_5 is possible, but it assumes that we have an a priori assumption on its location.

3.2.3. Estimation results in function of the number of activated sources

In this part, we present the results of the location estimation when the number of activated sources varies from two to four. The strength of the activated sources is equal to 25 W m^{-1}. The measurements are disrupted with an error of standard deviation equal to 0.1 °C. In the two cases, the middle heat source g_5 is activated and we observe the distortion of its confidence area, when the number of activate sources increases. As we can see in Fig. 14(a) the source situated in the center can be estimated with a good confidence interval when only one additional source is activated. The results displayed in Fig. 14(b) show an estimation problem with 3 additional sources. Indeed, in this configuration, the parameters of the middle heat source are correlated with those of the other sources, which explains the size of the obtained confidence ellipse. The results could be worse with five

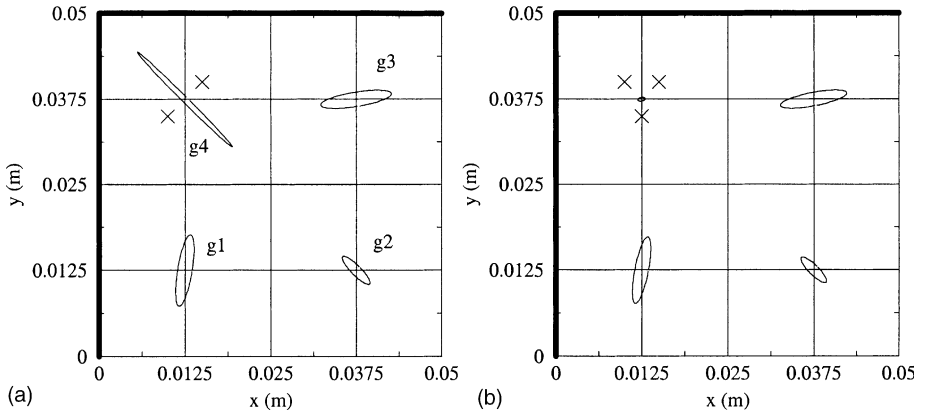

Fig. 13. Confidence ellipses obtained when the temperature and the heat flux are given on two closed faces (Γ_1 and Γ_2): (a) two additional internal sensors (×) and (b) three additional internal sensors (×).

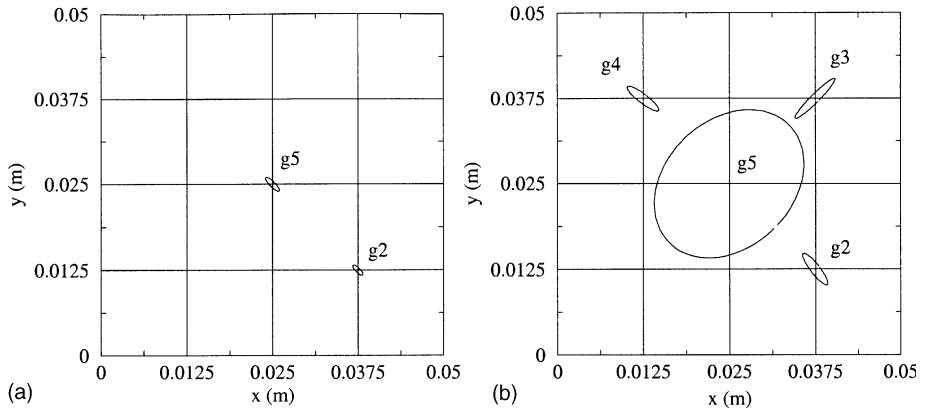

Fig. 14. Confidence ellipses obtained when the temperature and the heat flux are given on the whole boundary with $\sigma = 0.1$ °C: (a) g_2 and g_5 activated and (b) g_2, g_3, g_4 and g_5 activated.

sources, a configuration we did not manage to solve with our steady-state experiment of in [12].

3.3. Numerical simulation for non-symmetrical locations

In this part, we present an example based on the same geometry, but with four sources, which locations are not symmetrical within the bar. The four sources are activated with a same strength equal to 25 W m^{-1} and their location are displayed in Fig. 15(b). The corresponding direct temperature at the boundary versus the curvilinear co-ordinate is given in Fig. 15(a).

In Fig. 16, we present the estimated locations with 100 numerical simulations and the corresponding confidence area for each location. In this example, temperature and heat flux are known along the entire boundary and the measurements are disrupted with an error of standard deviation equal to 0.1 °C in (a) and 0.5 °C in (b). In the case (a), the estimated locations are all situated in the confidence interval. Source g_6, which is located very close to the boundary and far enough from the other sources, has a very small confidence ellipse.

For sources g_8 and g_9, the confidence interval is more important, although they are located closed to the boundary. As they are closed to each other, their parameters are correlated, which explains the size of their confidence ellipse. For source g_7, which is located in the middle of the square section, there is no problem of estimation in this configuration compare to the precedent case, although there are three additional sources too.

Concerning very poor measurements quality (see figure (b)), the confidence ellipses overlap each other and a lot of estimated locations are located outside the confidence ellipses. This last remark is important and shows that as the model is non-linear, we can only get an estimation of the confidence interval. This estimation

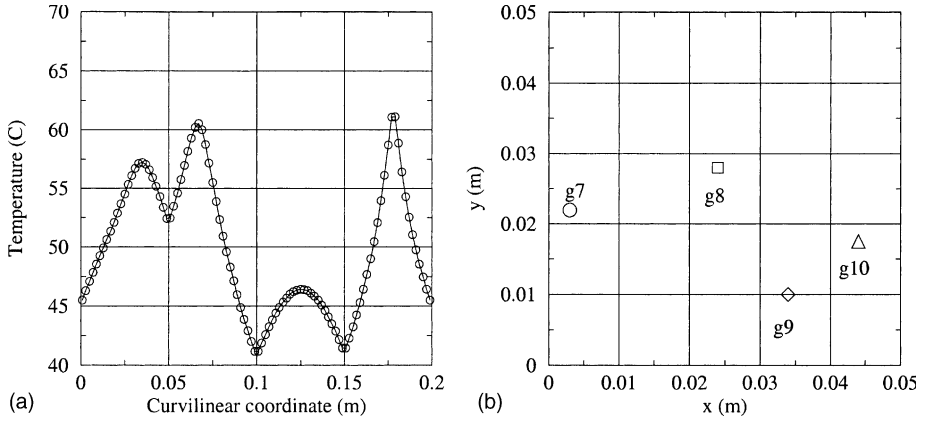

Fig. 15. (a) Temperature versus the curvilinear co-ordinate; (b) locations of the sources into the square bar ((○) g_7; (□) g_8; (◇) g_9; (△) g_{10}).

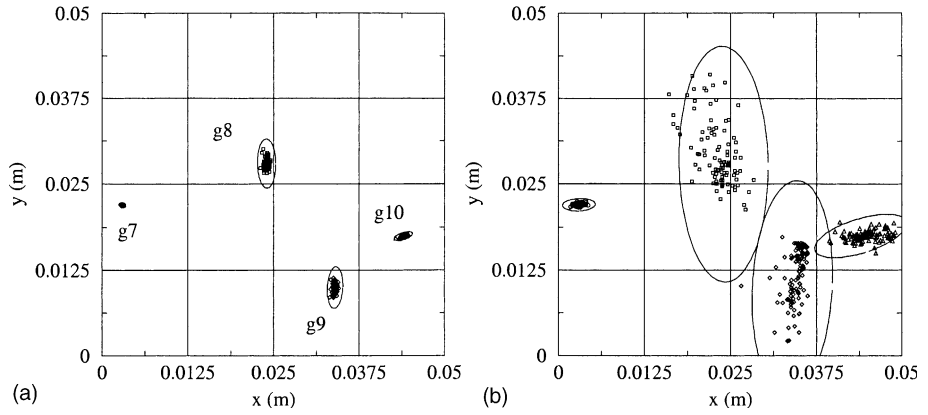

Fig. 16. Location estimation results for four source g_7, g_8, g_9 and g_{10} activated with the same strength equal to 25 W m^{-1}. Results for: (a) $\sigma = 0.1$ °C; (b) $\sigma = 0.5$ °C.

will be even less correct since the model is not linear around the solution.

4. Conclusion

In this paper, we have presented a parameter estimation for the identification of point heat sources in the steady case. Our method permits to obtain an estimation of the error on the results of the location and strength estimation of multiple point heat sources. This method can be applied to the steady case because the locations and strengths of the point heat sources can be considered as parameters of the mathematical model. In the transient case, these methods can not be applied because the strength is also a function of the time. As a result, the strength estimation procedure is a function estimation procedure instead of a parameter estimation procedure.

References

[1] T.J. Martin, G.S. Dulikravich, Inverse determination of boundary conditions and sources in steady heat conduction with heat generation, J. Heat Transfer Trans. ASME 118 (1996) 546–554.

[2] C.H. Huang, S.C. Cheng, A three-dimensional inverse problem of estimating the volumetric heat generation for a composite material, Numer. Heat Transfer A 39 (2001) 383–403.

[3] C.H. Huang, M.N. Özisik, Inverse problem of determining the unknown strength of an internal plane heat source, J. Franklin Instit. 329 (4) (1992) 751–764.

[4] A.J. Silva Neto, M.N. Özisik, Inverse problem of simultaneously estimating the timewise-varying strengths of two plane heat sources, J. Appl. Phys. 73 (5) (1993) 2132–2137.

[5] A.J. Silvaeto Neto, M.N. Özisik, Simultaneous estimation of location and timewise varying strength of a plane heat source, Numer. Heat Transfer A 24 (1993) 467–477.

[6] A.J. Silva Neto, M.N. Özisik, Two-dimensional inverse heat conduction problem of estimating the time-varying strength of a line heat source, J. Appl. Phys. 71 (1992) 5357–5362.

[7] C.Y. Yang, Solving the two-dimensional inverse heat conduction problem through the linear least-squares error method, Int. J. Heat Mass Transfer 41 (2) (1998) 393–398.

[8] C.Y. Yang, A sequential method to estimate the strength of the heat source based on symbolic computation, Int. J.Heat Mass Transfer 41 (14) (1998) 2245–2252.

[9] C.Y. Yang, The determination of two heat sources in an inverse heat conduction problem, Int J. Heat Mass Transfer 42 (1999) 345–356.

[10] G. Karami, M.R. Hematiyan, A boundary element method of inverse non-linear heat conduction analysis with point and line heat sources, Commun. Numer. Methods Eng. 16 (2000) 191–203.

[11] R. Abou Khachfe, Y. Jarny, Determination of heat sources and heat transfer coefficient for two-dimensional heat flow: numerical and experimental study, Int J. Heat Mass Transfer 44 (7) (2001) 1309–1322.

[12] C. Le Niliot, F. Lefèvre, A method for multiple steady line heat sources identification in a diffusive system: application to an experimental 2D problem, Int J. Heat Mass Transfer 44 (2001) 1425–1438.

[13] C. Le Niliot, F. Lefèvre, Multiple transient point heat sources identification in heat diffusion: application to numerical 2D and 3D problems, Numer. Heat Transfer B 39 (3) (2001) 277–301.

[14] F. Lefèvre, C. Le Niliot, Multiple transient point heat sources identification in heat diffusion: application to experimental 2D problems, Int J. Heat Mass Transfer 45 (9) (2002) 1951–1964.

[15] J.V. Beck, K.J. Arnold, Parameter Estimation in Engineering and Science, John Wiley and Sons, New York, 1977.

[16] M.R. Spiegel, Theory and Problems of Statistics, McGraw-Hill, New York, 1998.